Search for the Intermediate Vector Boson*

C. M. Ankenbrandt,† R. C. Larsen, L. B. Leipuner, and L. W. Smith
Brookhaven National Laboratory, Upton, New York 11973

and

P. J. Wanderer,‡ R. J. Stefanski,§ H. Kasha, and R. K. Adair
Yale University, New Haven, Connecticut 06520

(Received 17 December 1970)

A search for the vector boson (W particle), postulated as the mediator of the weak interaction, has been carried out by determining the intensity and polarization of muons originating very near the point of interaction of 28-GeV protons with nucleons. Bosons were not observed and the upper limit on the production cross section for W's with masses between 2.0 and 4.5 GeV/c^2 is $B\sigma_W \lesssim 6\times10^{-36}$ cm^2, where B is the branching ratio for the W decay to a muon and a neutrino. A comparison between the measured flux of muon pairs and the flux expected on the basis of a plausible model for the production and decay of both W's and heavy virtual γ's suggests that the experiment may not have been sensitive to W's, if they exist in this mass region. The flux of high-energy muons produced directly by an unknown process, an X process, is determined to be no greater than 10^{-6} times the pion flux.

I. INTRODUCTION

It is attractive to think that the weak interaction, like the strong and electromagnetic interactions, might be described in terms of the exchange of an intermediate particle. Such a particle would have unit spin in order to transmit the vector and axial-vector fields of the weak interaction[1]; further, experiment has established that it would be massive, and from the mass and known coupling, the particle must be short-lived. This paper reports the results of a search for this possible carrier of the weak interaction, the intermediate vector boson, or W particle. Preliminary results of this work have been published.[2]

Previous experiments have attempted to produce intermediate vector bosons with high-energy neutrinos. Such experiments are attractive because the cross section for this process can be reliably calculated. A neutrino may dissociate into a W and a muon, via the mechanisms depicted in Figs. 1(a) and 1(b), with momentum and energy being conserved through electromagnetic interactions with the nucleus. The W might be detected when it decays to a muon and a neutrino. Accelerator experiments[3,4] designed to detect neutrino-produced W's have yielded negative results, which are expressed as a limit on the mass, $M_W \geq 2M_N$, where M_W and M_N are the mass of the W and the nucleon, respectively. The flux of high-energy neutrinos was not large enough to produce observable numbers of W's with greater mass.

The measured flux of muons produced by cosmic-ray neutrinos has been compared[5] with the expected flux, which was estimated from data on the interaction of neutrinos at accelerator energies. Presuming a reasonable knowledge of the cosmic-ray neutrino spectrum, it is difficult to see why the muon fluxes are not substantially higher than measured if the W mass is as low as $5M_N$.

Nucleon-nucleon collisions have also been studied in an attempt to detect W's. Production mechanisms corresponding to the diagrams of Figs. 1(a) and 1(b) suggest that the intensity for the production of W's by neutrinos must be proportional to

$$I_\nu \sim g^2 e^2 e^2 F_{\gamma Z}^2(t),$$

while the equivalent factors for the production of W's in nucleon-nucleon interactions are

$$I_N \sim g^2 G^2 G^2 F_{pn}^2(t') F_{nN}^2(t''),$$

where $F_{\gamma Z}$, F_{pn}, and F_{nN} are the form factors governing the four-momenta, t, t', t'', transferred at the nucleon vertices. The coupling constants for the strong, electromagnetic, and weak interactions at the vertices are, respectively, $G^2 \approx 1$, $e^2 = 1/137$, and $g^2 = (10^{-5}/\sqrt{2})\,(M_W/M_N)^2$, where we have taken $c = \hbar = 1$. Assuming unit form factors, the intensity for production by nucleons may be as much as $(137)^2$ times the intensity for production by neutrinos. The intensity I_N is presumably reduced from this value by small form factors, but in the absence of detailed knowledge of the nucleon structure, the amount of the reduction is not known.

An experiment performed by a Columbia group[6] was concerned with a search for muons originating in proton-nucleon collisions in excess of those expected from meson decay. The decay of W's would constitute one possible source of such muons. Since muons produced in the decay of a heavy W are

more likely to have a large transverse momentum than those produced in the decay of the lighter π and K mesons, measurements were made out to large angles (10°) to maximize the signal-to-background ratio. Fluxes of muons with energy greater than 12.5 GeV, produced by 20-GeV/c and 30-GeV/c incident protons, were not in excess of those expected from meson decay. The experimental result, interpreted in terms of a particular, though plausible, model for W production and decay,[7] yielded

$$B\sigma_W \leq 5\times10^{-34}\ \text{cm}^2$$

for W's in the mass range ~3 to ~6 GeV/c^2, where B is the branching ratio for W decay into muon and neutrino and σ_W is the cross section for W production.

An Argonne-Wisconsin collaboration[8] examined the μ^- fluxes produced by 12.5-GeV/c incident protons, at 20° and in the momentum range 4 to 6 GeV/c, obtaining the negative result

$$Bd^2\sigma_W/d\Omega dp \leq 4\times10^{-34}\ \text{cm}^2/[\text{sr (GeV}/c)\ \text{nucleon}].$$

According to the W production model used, the experiment was sensitive to M_W in the range 2 to 2.5 GeV/c^2.

However, the uncertainties in the calculation of W production by nucleon-nucleon collisions are such that it is difficult to draw firm conclusions regarding the nonexistence of the W simply from the absence of a "muon excess." For example, electromagnetic processes are expected to contribute a muon flux comparable to the flux from W decay.[9] Since such a flux was not observed, it is likely that the previous proton-nucleon experiments were also insensitive to muons from W decay.

Although previous attempts to detect W's have yielded negative results, there are indications that the W mass may not be extremely large. Two models of weak interactions at low energies, the current-current model and the intermediate-vector-boson model, diverge at large energies. If a weak-interaction "cutoff" energy, Λ, is introduced, its size can be estimated.[10,11] Processes which are forbidden in first-order but allowed in second-order weak interactions place the tightest restriction on Λ. The branching ratio

$$(K_L \to \mu^+\mu^-)/(K_L \to \text{all})$$

is less than 3.8×10^{-9}, giving $\Lambda \lesssim 20$ GeV.[12] Estimates made of the matrix elements that account for the $K_L - K_S$ mass difference place Λ near 3–4 GeV.[13] The interpretation of Λ in terms of M_W depends in detail on the mechanism causing the cutoff,[14,15] but suggests that $M_W \lesssim \Lambda$.[16]

With these considerations in mind, we felt it important to attempt a more sensitive search for the W. The present experiment searched for W's produced in the interaction of 28-GeV protons with a uranium target. Muons travelling in the forward direction were charge-separated, slowed in a thick steel shield, and then stopped in a detector which observed both the incident muon and the subsequent decay electron. Measurement of the muon flux and polarization as functions of the density of the uranium target allowed muons from W decay to be distinguished from those produced by other sources. On the basis of our model for W production, the ex-

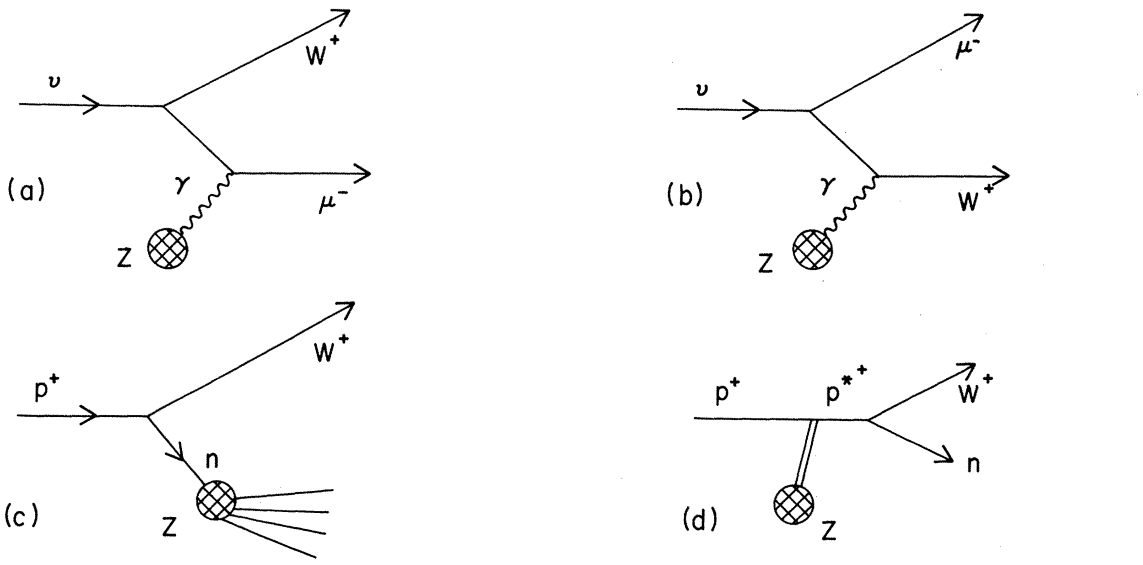

FIG. 1. Feynman diagrams of four mechanisms for W^+ production are shown. Production by neutrinos is depicted in (a) and (b). Part (c) shows a W^+ produced by the exchange of a baryon, and in part (d) the diagram for production by diffraction dissociation is presented.

periment was expected to be sensitive to muons from W's in the mass range ~2 to ~4.5 GeV/c^2.

II. THE FLUX AND POLARIZATION OF MUONS

A. General Characteristics

Intermediate vector bosons produced according to the mechanisms suggested in Figs. 1(c) and 1(d) should carry off most of the energy of the incident proton. A fraction B of them will decay into a muon and a neutrino and, if the decay is such that the muon is forward in the W center-of-mass system, the muon will also have a large laboratory energy. The experimental apparatus was designed to detect high-energy muons produced in the forward direction.

Further, muons from the decay of the W^+ will have longitudinal polarization very near +1. Positive muons produced in the decay of the massive W will be extremely relativistic and, therefore, expected to exhibit a helicity close to that of the antineutrino. Indeed, a calculation[17] of the polarization of the muon in the W center-of-mass system shows that it differs from +1 by terms which are on the order of M_μ^2/M_W^2, where M_μ is the mass of the muon. A muon with helicity +1 in the W center-of-mass system has a laboratory helicity[18]

$$P_{\text{lab}} = 1 - 2\frac{M_\mu^2}{M_W^2}\frac{E_W}{E_\mu}$$

in the limit $M_W \gg M_\mu$, where E_W and E_μ are the laboratory energies of the W and the muon. For the forward muons detected in this experiment, $E_\mu \cong E_W$, so muons which are produced in W decay and which stop in the detector will have longitudinal polarization >0.99.

Besides W's, three other sources of muons are expected to be the principal contributors to the flux of high-energy, forward muons: Muons will be produced through the weak decay of charged mesons (principally pions and kaons) and the electromagnetic decay of neutral vector mesons (ρ, ω, φ), and the decay of virtual γ's of large invariant mass will result in muon pairs. These last two sources are closely related; only a small momentum transfer is required to convert a virtual γ of the appropriate invariant mass into a ρ, and vice versa.

An otherwise unknown mechanism of muon production (X process) has been postulated to explain the results of measurements of cosmic-ray muons made by a group of physicists at the University of Utah. They find that their observations cannot be explained by assuming that all muons are produced by meson decay,[17] but the results are consistent with the hypothesis that about 2% as many muons are produced directly as pions for energies over 1000 GeV. It is implausible that so large a proportion should result from W production.[19] The results of the present experiment can be used to place a limit on the magnitude of this X process for 25-GeV muons produced from the interactions of 30-GeV

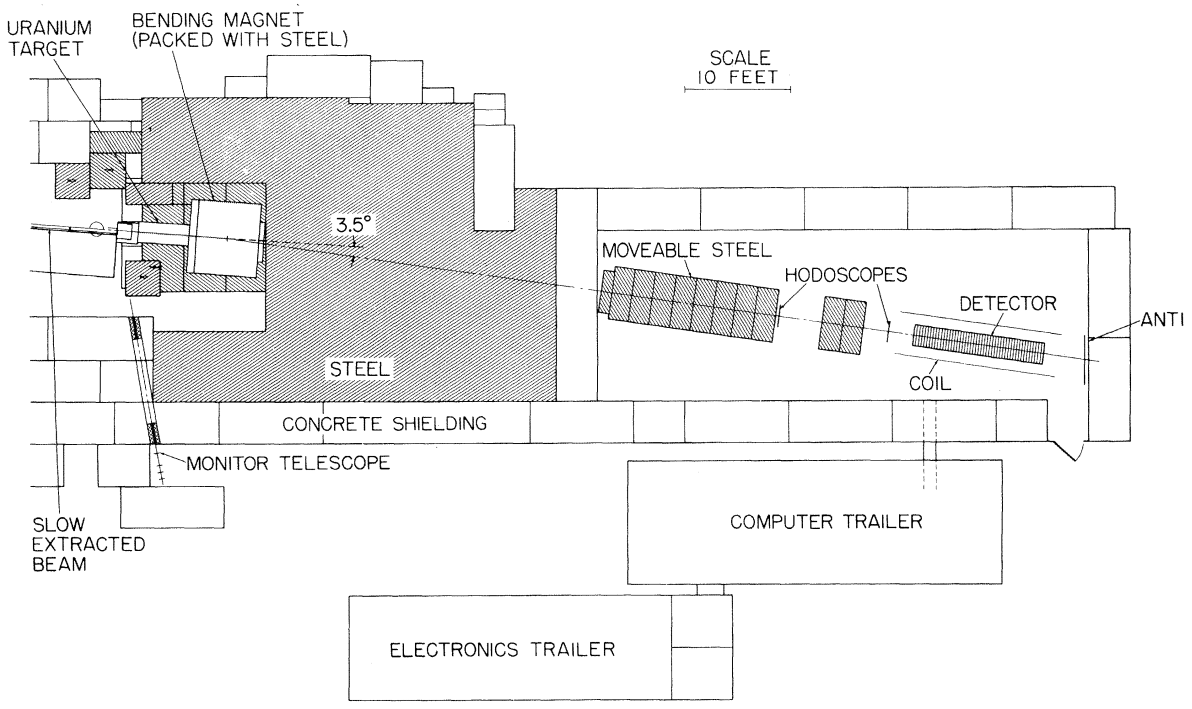

FIG. 2. Sketch of the experimental apparatus.

protons with matter.

In order to distinguish the W^+ contributions to the muon flux from those due to other processes, the experiment was constructed so that the μ^+ and μ^- could be examined separately. A bending magnet, located immediately downstream of the target, separated the positive and negative muon fluxes and directed one of them toward the detector, as shown in Fig. 2. The target was constructed so that its density could be varied. Measurement of the μ^+ and μ^- fluxes, and of the μ^+ polarization, as functions of target density, enabled possible W^+ contributions to the flux to be determined in two independent ways, by analysis of the positive and negative muon intensity as a function of target density, and by a measurement of the muon polarization as a function of target density. At all angles and energies, the flux of pions and K mesons produced in high-energy proton-nucleon collisions is certain to be much larger than any flux of W's similarly produced. However, the pion flux falls off rapidly as the energy of the pion approaches that of the incident proton. The flux of forward muons from the decay of a massive W^+, on the other hand, peaks at a relatively low energy (corresponding to muons which were backward in the W c.m. system) and at a very high energy (corresponding to muons which were forward in the W c.m. system). Hence, the ratio of W-produced muons to meson-produced muons should be maximized, in the forward direction, by examining muons whose energy is only slightly less than the energy of the incident proton.

If the incident proton beam strikes a very dense target, such as uranium, virtually all of the charged mesons will undergo a strong interaction before they decay. The interaction length for a pion in uranium is $\approx$12 cm, whereas the laboratory decay path for a 25.1-GeV pion is $\approx 1.4\times10^5$ cm. Since a single interaction will almost certainly remove the pion from the high-energy "tail" of the distribution, only $\approx10^{-4}$ of the total pion flux will contribute to the observed muon flux, if all of the incident beam interacts in the target. Similar considerations apply to K mesons.

If N is the number of muons which are produced in meson decay, in a uranium target of density 1 (relative to the density of solid uranium), then $2N$ muons will be produced in a dispersed uranium target of density $\frac{1}{2}$ the maximum density (since the pion interaction length is now $\approx$24 cm). Similarly, $3N$ will be produced in a uranium target of relative density $\frac{1}{3}$. Linear extrapolation of a plot of muon flux versus the reciprocal of the target density, to infinite target density, then eliminates the meson contribution to the muon flux, and yields the muon flux due to the "prompt" decay ($\lambda_{\text{decay}} \ll \lambda_{\text{interaction}}$) of a parent particle formed in the initial proton-nucleon interaction. A flux of "prompt" negative muons will then be evidence for the production of muon pairs, and subtraction of this flux from the μ^+ "prompt" flux gives the muon contribution due to W^+ decay. We presume that the flux of W^- will be much less than the flux of W^+.

When a spin-0 meson (such as a pion or K meson) decays to a muon plus neutrino, angular momentum conservation requires that the spins of the two leptons be oppositely directed. If the meson has a positive charge, a neutrino with helicity -1 will be produced, so the helicity of the positive muon will be -1 also. In the laboratory, forward muons from meson decay will therefore have longitudinal polarization -1. The electromagnetic decays of neutral particles conserve parity, so the muons produced in these decays will have zero average polarization. Hence, a change in polarization with target density is evidence of a muon flux which originates in the decay of neutral particles or W's, and which is comparable in size to the flux of muons from meson decay. The character of such effects is suggested by the graphs of Fig. 3.

B. Flux Estimates

Diagrams which are expected to be important in the production of high-energy W^+ bosons in nucleon-nucleon collisions are sketched in Figs. 1(c) and 1(d). The diagram of Fig. 1(c) corresponds to a process that takes place via baryon exchange, and

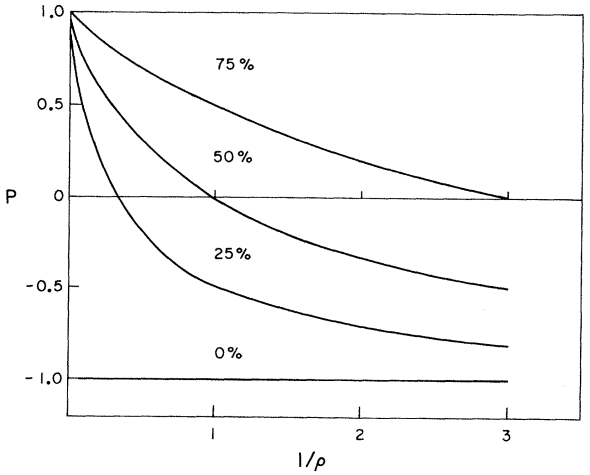

FIG. 3. The polarization P of a flux of muons composed of forward muons from the decay of charged mesons (with $P=-1$) and forward muons from W decay (having $P=+1$) is shown as a continuous function of inverse target density $1/\rho$, where ρ is taken as 1 for solid uranium. The fraction of the flux corresponding to muons from W decay, at target density 1, varies from zero (the lowest of the four curves shown in the figure) up to 75% (the top curve).

Fig. 1(d) describes W production by diffraction dissociation. It was felt that the two mechanisms might be of comparable importance in producing W's with 28-GeV protons, if the mass of the W is between 2 and 4.5 GeV/c^2. The interference between 1(c) and 1(d), or other possible W production mechanisms, is likely to be small, so it might be hoped that the general features of the energy and angular distributions of W's produced in nucleon-nucleon interactions might be obtained from a detailed calculation of the process depicted in Fig. 1(c). An estimate of W production via diagram 1(d) is also made.

A technique developed by Chew and Low[20] was used in calculating the flux corresponding to Fig. 1(c). A process typical of those to which this technique is applied is the reaction $\pi N \to \pi\pi N$ shown in Fig. 4(a). The amplitude is assumed to be dominated by a pole which occurs when the square of the invariant mass of the virtual particle exchanged in the process, Δ^2, is equal to the square of the mass of the physical particle,

$$A(\Delta^2) \sim 1/(\Delta^2 - M_\pi^2),$$

where M_π is the pion mass. The momentum transferred to the "spectator" particle, the nucleon, is small, and is treated nonrelativistically. The calculation relates measurements of the momentum and angle of the recoil "spectator" particle to the total π-π cross section.

The Feynman diagram of Fig. 1(c) is redrawn in Fig. 4(b) to correspond to the process discussed by Chew and Low; in this reference frame, the incident proton is at rest. The incident "spectator" proton exchanges a baryon number and is transformed into a W^+. Since the W is moving slowly in the frame of the incident proton, it will have a laboratory energy nearly equal to the energy of the incident proton. Here, the total nucleon-nucleon cross section gives information about the energy and angular distributions of the W^+.

Given a specific mass for the W, the production cross section is determined in terms of Δ^2 and ω^2, the square of the invariant mass of the system of the virtual nucleon and the spectator nucleon. The cross section is then

$$\frac{d^2\sigma}{d(\Delta^2)d(\omega^2)} = \frac{U^2}{2\pi}\frac{M_W}{M_N}\frac{(\frac{1}{4}\omega^4 - \omega^2 M_N^2)^{1/2}}{Q^2}\frac{\sigma(\omega)}{(\Delta^2 - M_N^2)^2}, \tag{1}$$

where $\sigma(\omega)$ is the nucleon-nucleon cross section at energy ω, Q is the momentum of the incident proton, and U is the matrix element for the $\langle p, n, W\rangle$ vertex. The matrix element was determined from the conserved-vector-current theory (CVC), which relates this weak-interaction vertex to the corresponding electromagnetic vertex, $\langle p, n, \gamma\rangle$, by specifying that the matrix element for the vector part of the weak interaction is equal to the matrix element for the isovector part of the electromagnetic interaction, apart from numerical factors involving Clebsch-Gordan coefficients and the Cabibbo angle, which are not much different from 1. Presuming that there is no strong difference between the vector and axial-vector contributions to W production, or between the isoscalar and isovector portions of the electromagnetic current, the matrix element may be taken as the electromagnetic matrix element,

$$4\pi U^2 = \frac{g^4}{4M_N^2}\,|(p_i + p_\nu)(p_\mu - p_\nu)|^2 \times \int \frac{dq^2}{|(M_W - i\Gamma/2)^2 + q^2|^2}, \tag{2}$$

where p_i and p_ν are the four-momenta of the incident proton and the virtual nucleon, and p_μ and p_ν the four-momenta of the muon and the neutrino produced in the decay of the W. The W decay width Γ is equal[9] to $g^2 M_W^2/6\pi B$, where B is taken[21] as $\frac{1}{4}$. The matrix element averages over the several possible spin configurations of the system by treating the nucleons as scalar particles.

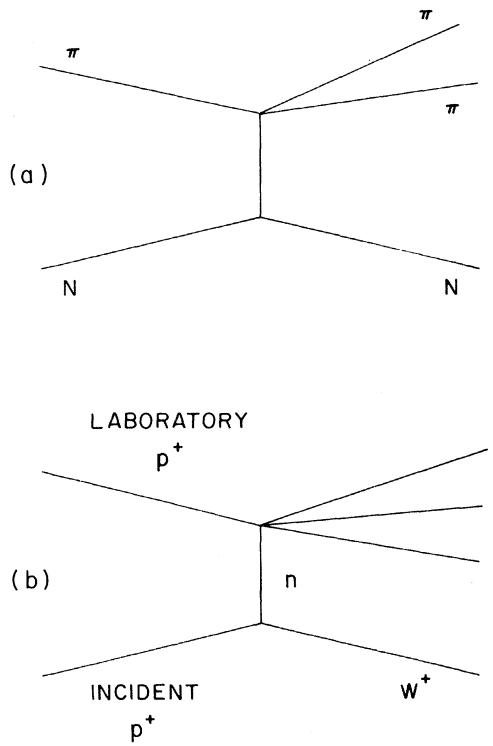

FIG. 4. The Chew-Low method of analysis is typically applied to reactions such as that depicted in part (a) of the figure. The W-production mechanism of Fig. 1 (c) is redrawn in part (b) of this figure, in order to illustrate its relation to reactions such as that shown in part (a), and the applicability of the Chew-Low technique.

The expression (1) describes W production in the idealized case where the two vertices involve point particles and the virtual nucleon exchanged in the reaction is close to the mass shell (i.e., $\Delta^2 - M_N^2$ is small). Allowance must be made for the extended structure of the nucleons and the distance of the pole from the physical region.

The matrix element U [Eq. (2)] describes the production of W's from a point charge. A form factor F, multiplying U, takes into account the structure of the nucleon. Here, F is taken as an average of the separate form factors which are related to the distributions of the charge and magnetic moment in the nucleus. As with the matrix element, the weak-interaction form factor for the nucleon is related to the electromagnetic form factor through the CVC hypothesis. Little is known of the nucleon structure in the region of timelike four-momentum transfer $q^2 = -M_W^2$, but experiments[22] have set upper limits on the vector form factor:

$$F \leq 0.2 \text{ for } q^2 \approx -5 \text{ to } \approx -6 \text{ (GeV}/c)^2.$$

Further, it should be noted that the process described by expression (1) involves only one intermediate state – that of the virtual neutron. A complete calculation of W production requires a summation over all possible intermediate states. We combined our ignorance of the value of this summation as well as our ignorance of the behavior of the form factor by taking $F = 1$ in the calculation. There is substantial reason to think that this approximation may not be unrealistic. Recent experiments[23] have found that the cross section for "deep"-inelastic electron-proton scattering,

$$e + p \rightarrow e' + \text{anything},$$

falls off very slowly with increasing momentum transfer. It has been suggested[24] that the data may be explained in terms of the recently proposed "parton" model of Feynman,[25] where the electron scatters, not from a "soft" nucleon, but from a nucleon made up of pointlike partons, making large spacelike momentum transfers possible. Similarly, it may be possible to transfer a timelike four-momentum-squared equal to $-M_W^2$ with a form factor equal to 1, when all possible intermediate states are considered.

Experimental evidence[26] suggests that the form factor which describes the virtual-neutron–target-nucleon vertex behaves like e^{-3t}. Here, t is the absolute square of the minimum four-momentum transfer necessary to push the virtual neutron back onto the mass shell. This form factor does not affect the cross section very much.

Expression (1) describes a reaction which takes place via a single intermediate state, as previously noted, and will accurately represent the behavior of the cross section only in the region near the singularity at $\Delta^2 = M_N^2$. The process considered here is rather far from the pole (Δ^2 is typically $\approx -M_N^2$), and it is necessary to consider a modification of this form. A study[26] of ρ production in the very similar reaction

$$p + p \rightarrow d + \rho, \tag{3}$$

where the momentum of the incident proton was 21.1 GeV/c, indicates that the cross section is modified by a factor of the form

$$\exp[B(s)(\Delta^2 - M_N^2)],$$

where s is the square of the center-of-mass energy. By choosing $B(s) = 0.9 \ln s$, we have a Regge form[27] for the factor, and obtain cross sections consistent with the measurements made on reaction (3). For values of Δ such that reaction (3) is kinematically allowed, the form factor is very small. The smallness of the form factor may, however, be considered as a consequence of the restriction to one final state, the deuteron, in reaction (3). Since our experiment accepts all final states in W production, our use of this form factor for W production is likely to result in a very conservative estimate of the W-production cross section.

It was assumed that the W's were unpolarized and therefore decayed isotropically. However, some small degree of polarization is possible. The $V - A$ form of the weak interaction favors interactions of positive-helicity states of the neutron and the proton, just as preference is shown for positive-helicity states of the μ^+ and the e^+. If we consider the proton, with a spin component of $\frac{1}{2}$ in the beam direction, "decaying" to a neutron going backwards and a W^+ going in the beam direction, it is clear that the W^+ will have a tendency to be polarized, so that the component of spin in the beam direction will be +1. The W decay will then favor an arrangement of lepton spins such that the component of angular momentum is +1 in the direction of motion of the W. Such a configuration is obtained if the muon is emitted in the forward direc tion and the neutrino to the rear. Thus, the existence of a partial W polarization should enhance the sensitivity of the experiment. But when very high energy W's are produced, the neutron goes forward or backward in the c.m. system with very little momentum and, hence, very little bias toward a definite helicity. Such high-energy W's will not be strongly polarized, and the effects of any W polarization will be small.

The momentum transfers required for the production of W's are large enough for the process to be dominated by nucleon-nucleon interactions, and any production via a mechanism requiring a coherent interaction between the protons and the nucleus

is small.

The Fermi momentum of the nucleons in the uranium nucleus can have an important effect on W production if the mass of the W is near the kinematic limit. The heaviest W that can be produced by a 29-GeV/c proton colliding with a stationary nucleon is 5.7 GeV/c^2. If the target nucleon has a momentum of 300 MeV/c, a typical value, and is moving in the opposite direction to the incident proton, a W as massive as 6.9 GeV/c^2 can be produced. More generally, the Fermi momentum increases the phase space available for the production of particles with mass near the kinematic limit, and hence makes the experiment more sensitive if the W mass is close to this value. The Fermi momentum of the nucleons also broadens the energy and angular distributions of the W's, but this broadening is small compared with that due to the effects of multiple scattering and straggling of the muons.[28]

The results of this calculation of W production, presented in terms of the energy and angular distributions of the decay muons expected for $M_W = 3$ GeV/c^2, are given in Fig. 5. Total cross sections for several values of M_W are given in Table I.

It is useful to estimate the total cross section for W production via diffraction dissociation, as depicted in Fig. 1(d). We assume that the ratio of W production to pion production is approximately the same as the ratio of the relative probabilities for finding a W and a pion in the field of the nucleon, which we estimate as

$$\frac{\sigma_W}{\sigma_\pi} \approx \left(\frac{g^2}{G^2}\right)\left(\frac{\lambda\!\!\!^{-}_W{}^3}{\lambda\!\!\!^{-}_\pi{}^3}\right),$$

where the Compton wavelengths are

$$\lambda\!\!\!^{-}_W = \hbar/M_W c \quad \text{and} \quad \lambda\!\!\!^{-}_\pi = \hbar/M_\pi c,$$

and the total cross section for pion production, σ_π, is approximately 3×10^{-26} cm^2. As with the calculation of W production by baryon exchange, Fig. 1(c),

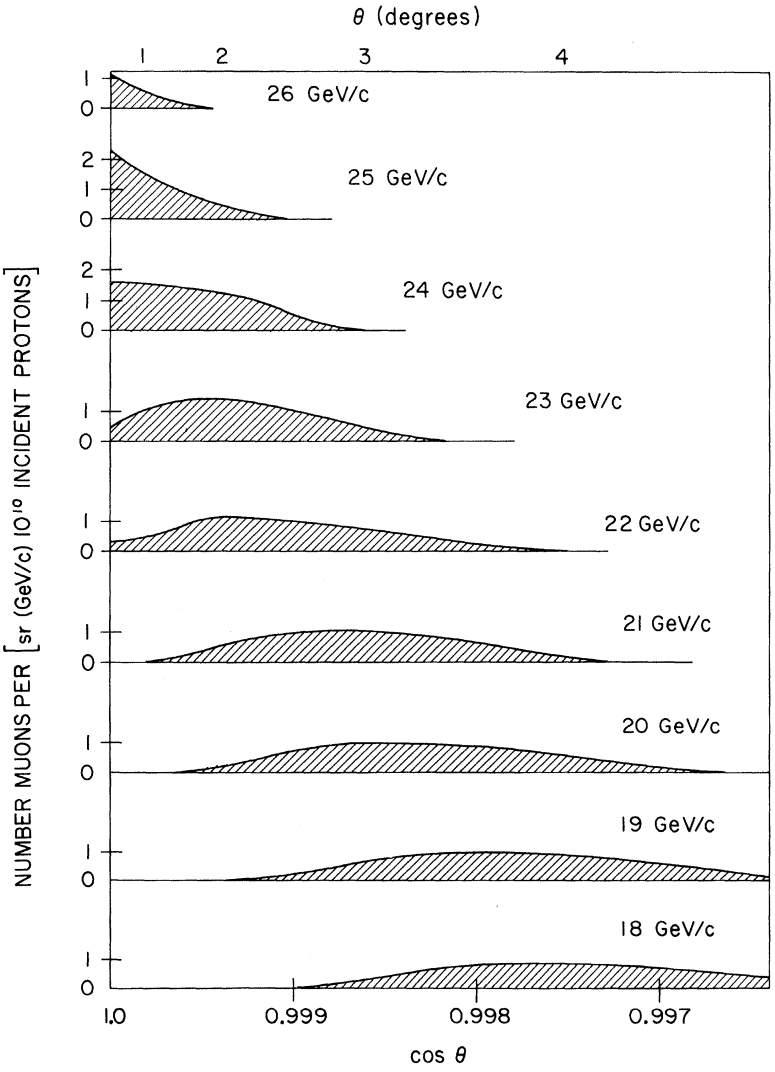

FIG. 5. This figure presents the results of our calculation of W production and decay according to the mechanism depicted in Fig. 1(c). The expected muon flux is given as a function as a function of angle, for nine different values of muon momentum. The mass of the W was taken as 3 GeV/c^2, and the branching ratio for muon decay, B, was assumed to be $\frac{1}{4}$. The experiment detected muons which had momenta near 25 GeV/c and which were produced near zero degrees.

the extrapolation from the production of a zero-mass boson, where the coupling constant g^2 is defined, to the production of a W with a finite mass, is governed by the nucleon form factor in the time-like region. Again the behavior of F and the summation over all possible intermediate states are approximated by taking $F=1$.

If $M_W = 3$ GeV/c^2, we obtain a value for σ_W of 6×10^{-36} cm^2 for W production via baryon exchange and 2×10^{-34} cm^2 for W production by diffraction dissociation. Values of the cross sections for other W masses are presented in Table I. It is perhaps not surprising that the diffractive production of W's, which is described in terms of the exchange of a Pomeranchuk trajectory and is expected to be energy independent, is much larger than W production by baryon-exchange processes, which is expected to decrease with increasing energy.

These two estimates of W production, together with the calculation of the energy and angular distributions of the decay muons for process 1(c), indicate that measurable fluxes of W's in the mass range 2 to 4.5 GeV/c^2 may be produced, and that a certain fraction of the decay muons will have large energies and small transverse momenta in the laboratory.

We also estimate the background flux of muons from meson decay and from electromagnetic pair production. Formulas developed by Sanford and Wang,[29] and by Hagedorn and Ranft,[30] were used in estimating the flux of muons due to meson decay. A detailed estimate of this flux is made in Sec. IV.

Estimates of the expected background due to muon pairs may be made in several ways. Using the relationship established by CVC, Yamaguchi[9] was able to estimate the ratio between the flux of muon pairs due to heavy virtual γ's with an invariant mass of q^2, produced by the isovector electromagnetic current and the flux of W's with a mass $M_W = q^2$, produced by the vector part of the weak interaction:

$$\frac{d\sigma_W}{d\sigma_e} \leq \left(\frac{M_W}{10M_N}\right)\left(\frac{M_W^2}{dq^2}\right), \tag{4}$$

where dq^2 represents the experimental resolution in the square of the mass of the W. For a 3-GeV/c^2 W and a mass resolution $\approx$2 GeV/c^2, this gives

$$d\sigma_W \lesssim \tfrac{1}{4} d\sigma_e .$$

If this relationship is not greatly affected by the axial-vector or isoscalar currents, and if M_W is near to 3 GeV/c^2, then the W-decay flux of muons is expected to appear with a comparable background due to muon pairs.

TABLE I. Estimates of W production from the processes of Figs. 1(c) and 1(d).

M_W (GeV/c^2)	σ_W from Fig. 1(c) (cm^2)	σ_W from Fig. 1(d) (cm^2)
2.0	3.7×10^{-35}	2.9×10^{-34}
2.5	1.9×10^{-35}	2.3×10^{-34}
3.0	6.3×10^{-36}	1.9×10^{-34}
3.5	1.3×10^{-36}	1.6×10^{-34}
4.0	9.9×10^{-38}	1.4×10^{-34}
4.5	1.9×10^{-39}	1.3×10^{-34}

This estimate agreed with the results of a calculation of the production of heavy virtual γ's via a baryon-exchange mechanism similar to that sketched in Fig. 1(c), with the appropriate matrix element used in place of the matrix element in expression (2).

The measurements[26] made on reaction (3) revealed approximately equal amounts of π^+ and ρ^+ production, suggesting that ρ^0 and π^+ fluxes in our experiment are likely to be comparable. Approximately 10^{-4} of the pions produced in the maximum-density target will decay to muon and neutrino, compared with the branching ratio for ρ decay to muon pairs, which has been measured[31] to be $(6\pm1)\times10^{-5}$. Thus, the flux of muon pairs from ρ decay is expected to be comparable both to the flux of muons from meson decay and to the possible flux of muons from W decay.

The principal contributions to the muon flux from neutral mesons, aside from the decays of the ρ which were included in the discussion of virtual γ's, are from the decay of neutral pions to two γ's. The γ's may then interact in the target to produce muon pairs. It is convenient to discuss this background by comparing it to the background expected from the decay of the π^+.

At high energies, the flux of positive pions is about twice the flux of neutral pions. Further, while the momentum spectrum of the muons from π^+ decay is degraded due to the energy taken off by the neutrinos, the spectrum of muons from the decay of the π^0 is degraded twice: when the energy of the π^0 is divided between the two γ's, and when the energy of a single γ is divided between the two muons. Finally, the ratio of muon pairs to electron pairs produced by the γ's is about $(M_e/M_\mu)^2 \cong 2.5\times10^{-5}$. This is to be compared to the attenuation of the π^+ flux which takes place in the uranium target, to 10^{-4} of its initial value. Since the π^0 lifetime is $\cong 10^{-16}$ sec, essentially all the neutral pions decay before interacting. All considered, it would appear unlikely that the high-energy muon flux from neutral pions is as large as one percent of the muon flux due to the decay of positive pions.

C. "Anomalous" Muons

Muons may be produced by the X process postulated to explain muon spectra in cosmic rays.[17]

The effect is observed at much higher muon energies, but in the absence of any knowledge of the nature of the process, it is impossible to impose an energetic threshold on its occurrence. A small effect at moderate cosmic-ray muon energy would escape detection. While it is impossible to predict the contribution of such an X process to the muon flux in the present experiment, the results of the experiment do serve to establish a limit on the contribution from this source.

D. Production Outside the Uranium Target

Experimentally, it is necessary to take account of the proton interactions which do not occur in the uranium target. It is relatively easy to calculate meson production in the small amounts of material (e.g., the proton-beam monitors) located immediately upstream of the uranium target. These corrections are discussed in detail in Sec. IV. It is also possible that a small fraction of the proton beam may strike the vacuum pipe far upstream of the target, and produce a background flux of muons from meson decay that cannot be readily calculated. Such a background would be independent of target density and would have the same positive-to-negative charge ratio as mesons produced in the uranium target. Unlike the flux of positive muons from W decay, the background would be larger at lower muon energies than at higher muon energies. The information from muons of lower energies then may be examined for the presence of this background and used to estimate the significance of a flux of prompt, positive muons in excess of the flux of prompt, negative muons.

III. EXPERIMENTAL DESIGN

A. Experimental Arrangement

The experimental apparatus is sketched in Fig. 2. About 10^{12} 28-GeV protons were extracted from the alternating gradient synchrotron at Brookhaven National Laboratory each accelerating cycle and directed onto the target. The extraction took place over a period of ≈ 200 msec.

The incident protons struck one of three uranium targets, which were constructed to have densities 1, $\frac{1}{2}$, and $\frac{1}{3}$, relative to the density of solid uranium. Each target was composed of 20 1-in.-thick uranium bricks. Targets of relative density $\frac{1}{2}$ and $\frac{1}{3}$ were made by leaving 1-in. and 2-in. gaps between the bricks. These "granular" targets were effectively equivalent to continuous targets of the desired densities.

A 6-ft-long bending magnet was located immediately behind the target. The gap of the magnet was filled with steel in order to provide an absorber for pions and protons that did not interact in the target. The magnet was set to deflect muons of the desired energy 3.5°, so that the muons arriving at the detector would be primarily of one sign. Particles of the opposite sign were obtained by reversing the magnetic field. The highest value of the magnetic field needed in the experiment was about 20 kG. This value was calculated[32,33] to within 5%, which was sufficient accuracy since the actual muon energy was determined from the amount of steel degrader in the beam.

Following the magnet, a 29-ft-thick steel shield was constructed. Virtually all secondaries, except for high-energy muons and neutrinos, stopped in the 35 ft of steel absorber that followed the target.

Forward-going muons, greatly slowed after passing through the steel absorber, next passed through four feet of concrete, which formed the front wall of a blockhouse, constructed around a final segment of steel and the detector. The blockhouse provided shielding from cosmic rays and low-energy neutrons.

After passing through the front wall of the blockhouse, the muons entered a series of steel blocks: a 1-ft-thick block, followed by as many as eight 2-ft-thick blocks. Changing the amount of this "movable" steel enabled the energy of the muons which stopped in the detector to be varied.

Muons exited the movable steel to pass through a hodoscope located 17 ft downstream of the concrete wall. A second hodoscope was 10 ft beyond the first, and between the two hodoscopes was a 4-ft-thick block of steel. The hodoscopes, as well as the detector, were 3 ft high and 2 ft wide. Each hodoscope was composed of vertical and horizontal counters arranged to divide the area into 1-ft-square sections. Particles which traversed the 1-ft-square section of the second hodoscope that was directly behind the 1-ft-square section they crossed in the first hodoscope, satisfied a "tight" angular requirement. All other particles which passed through both hodoscopes satisfied a "loose" requirement.

Data were taken with 13 ft, 9 ft, and 1 ft of movable steel, corresponding to 25.1-, 23.5-, and 20.3-GeV muons stopping in the detector.

Data on 11.6-GeV muons were also obtained, with no movable steel, 2 ft of steel between the hodoscopes, and a 16-ft-thick, 6-ft-wide section of steel removed from the downstream end of the absorber. Since the flux of secondary particles produced by the incident protons is much higher near 11.6 GeV than at energies above 20 GeV, the intensity of the proton beam was reduced while muons of this energy were being examined. This permitted the acquisition of data at approximately the same rate as at the higher energies, while the

background was reduced as much as possible.

B. Detector

The muon detector was composed of 24 $\frac{1}{4}$-in.-thick plastic scintillators alternated with 23 4-in.-thick slabs of aluminum. Each slab of aluminum and scintillator in the detector was 2 ft wide and 3 ft high. The upstream face of the detector was $2\frac{1}{2}$ ft from the second hodoscope. Two RCA 8575 photomultipliers collected light from each scintillator. The signals from the phototubes were passed through discriminator circuits and the logical AND of the resultant pulses was taken as the signal from the scintillator. The efficiency was $\geq 99\%$. The stopping power of the detector was taken as the difference in the initial energies of muons which stopped in the first slab and in the last slab of the detector. Since the rate of energy loss is a function of energy, the stopping power of the detector varies slightly with energy, from 1.45 GeV for 25.1-GeV muons to 1.39 GeV for 11.6-GeV muons.

A large array of scintillators, 5 ft wide and 6 ft high, was set up 6 ft downstream from the detector to serve as an anticoincidence counter. Pulses from the last scintillator in the detector were also included in the anticoincidence signal. The anticoincidence counters rejected particles whose energy was so large that they passed through the detector, and also eliminated a fraction of the particles which scattered out the sides of the detector. Most "tight" particles not stopping in the detector struck one of the anticoincidence counters. If a particle satisfied a "tight" angular requirement, and no pulse was detected from the anticoincidence counters, a "tight" trigger pulse (T) was generated; "loose" triggers (L) were generated similarly. The triggers were used to initiate acquisition of data by an on-line computer. Use of the anticoincidence counters in the triggering logic permitted exclusion of many of the particles which would have yielded no polarization information. This was of some importance, since the computer could only handle 50 triggers per pulse and the flux of incident particles was much larger during the measurements of the lower-energy muons.

Acquisition of data was further optimized by using the L trigger when there were fewer than 50 triggers per AGS cycle (to increase the trigger rate), and the T otherwise (since the ratio of muons stopping in the detector to muons scattering out of the detector is larger for T than for L).

The muon polarization is determined by measuring the direction of emission of the electron from the muon decay. A muon which stops in a given aluminum plate will emit an electron at some time τ after the muon stops, which may trigger the counter F further downstream or the counter B upstream of the plate. The component of polarization of the stopped muons along the beam direction at time τ will be proportional to the ratio

$$[N_F(\tau) - N_B(\tau)] / [N_F(\tau) + N_B(\tau)],$$

where $N_F(\tau)$ and $N_B(\tau)$ are the numbers of forward and backward electrons recorded at the time τ.

In order that the measurement of the muon's longitudinal polarization be as free as possible from experimental biases, a uniform, constant magnetic field directed perpendicular to the path of the incoming muons was imposed on the detector. A magnetic field will precess the muons at the frequency $\omega = geH/M_\mu c$, so the component of the polarization along the axis of the detector varies as a sinusoidal function of time. Biases, such as that caused by muons which stop in the scintillator instead of the aluminum, then appear as a constant added to the sine wave. A frequency $\omega \approx 2\pi/\tau_\mu$, where τ_μ is the muon lifetime, was chosen in order to determine both the maximum and the minimum of the sine wave as accurately as possible. The magnetic field was produced by a pair of rectangular coils, 140 in. long, 70 in. high, and separated by about 40 in. The current in the coils was constant to within 0.3% during the experiment, and maintained so that $\tau_{\text{precession}} = 2\pi/\omega$ had a value of 2.64 μsec at the center of the coil. The calculated field magnitude varied little over a given aluminum slab (typically 2%), and its direction was very nearly perpendicular to the beam (only $\approx 1\%$ of the total magnitude of the field was parallel to the beam). The field decreased by $\approx 5\%$ from center to front and back in the detector, and this change was taken into account in the analysis.

C. Data Acquisition

An on-line computer was used for the collection and partial analysis of the data as well as for constant monitoring of the experiment. A PDP-8 computer was used with a memory of 8K of 12-bit words, a scope, and a magnetic-tape unit. The connection between the experimental equipment and the computer was made through an interface which performed certain logical functions. The interface was responsible for sorting information from the detector according to whether it pertained to the incident muon or the decay electron, for obtaining information on the decay time of the muon, and for storing the resultant data in the computer. A trigger pulse (T or L) performed three functions in initiating data acquisition:

(a) The trigger generated a pulse about 20 nsec wide. Coincidences between this pulse and the pulses characterizing the muon's path through the hodoscope and the detector were then recorded in a set of buffer discriminators. A pulse from the

electronic logic, if accepted by a buffer discriminator, appeared as a logical "1" at the output, until read by the computer. If no pulse was fed to the buffer discriminator, the computer read "0," as depicted in Fig. 6. After the levels of the buffer discriminators were read by the computer, they were reset to "0."

(b) The trigger turned on the data interface, which scanned the detector pulses for a "$5\bar{3}$"-i.e., pulses from five consecutive scintillators followed by three scintillators without pulses, as shown in Fig. 6. The muon was assumed to have stopped in the aluminum slab immediately downstream of the last of the five scintillators. Simultaneously, a clock with at a least count of 0.1 μsec was started. For each of the two scintillators just upstream and the two scintillators just downstream of the aluminum slab where the muon "stopped," the time of the first pulse after the muon pulse was noted by reading the 0.1-μsec clock (t_1 through t_4 in Fig. 6).

(c) The T or L trigger was delayed by 0.3 μsec, and then it turned on a second rank of buffer discriminators which recorded the "electron" information by noting, for each counter in the detector, whether or not a pulse occurred between 0.3 μsec and 12.7 μsec. By recording all counters in the detector during this time period, useful information on backgrounds was obtained.

After 12.7 μsec, the contents of both ranks of buffer discriminators, the readings of the clocks, and the time in the AGS cycle at which the trigger occurred (to the nearest millisecond), were read into the memory of the computer. The complete

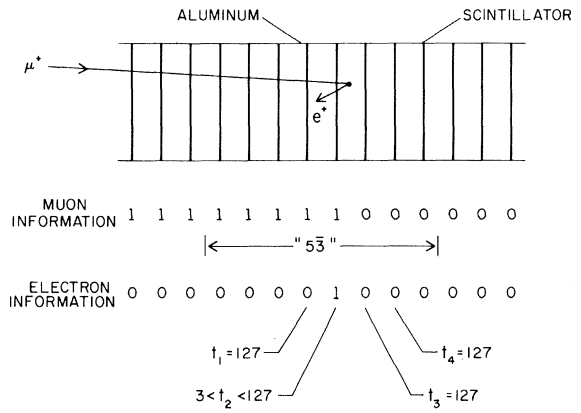

FIG. 6. A section of the muon detector is shown, not to scale. An incident muon stops in the detector, producing a decay positron directed backwards with respect to the muon direction. The decay occurs at a time t such that $3 \leq t \leq 127$, in units of 0.1 μsec. The section of the detector that satisfies the "$5\bar{3}$" criterion defined in the text is noted. The muon and electron information, as well as the times of pulses seen in the scintillators near the stopping point of the muon, are shown as recorded by the computer.

data acquisition took approximately 60 μsec. Any further triggers occurring during this time were ignored.

Data were collected only during the 200-msec period of each AGS cycle in which the proton beam was directed at the target. The computer could accommodate the data from 50 triggers per AGS cycle. Subsequent data, if any, were not recorded, although the total number of both T and L triggers was counted. At the end of the 200-msec period, the computer recorded eight scalers and three analog devices which monitored the number of incident protons, the number of muons, and the amount the proton beam "scraped" against the vacuum pipe. This monitor information, together with the data fed to the computer by the interface, was then written on magnetic tape which was saved for final, off-line, analyses of the data.

There were three monitors of the proton beam. The principal monitor was a four-fold coincidence telescope set at approximately 80° to the incident beam. Through a small hole in the shielding it viewed secondaries produced when the proton beam hit a thin aluminum vacuum window at the end of the beam pipe. A secondary emission chamber, located about 170 ft upstream of the target, was used as the reference monitor. It had been previously calibrated to within ±10% by foil activation,[34] and the calibration agreed with the estimates that had been made for the efficiency of extracting the beam from the ring of the AGS. This efficiency was expected to be between 70% and 90%. The signal from the chamber was digitized by two separate devices, and the output of both was recorded on our scalers. Our own digitization of the signal was also recorded. The third proton monitor was obtained by summing the signals obtained when the beam passed between two vertical plates. The pair was centered on the beam vertically, and the horizontal positioning was such that the difference of the two signals was an indication of the left-right centering of the beam, and was recorded and also used as part of a servo-loop that kept the beam centered on the target.

The number of muons produced each AGS cycle was determined through the number of T and L triggers, which were recorded on scalers. At the highest energy, there were about ten L triggers per AGS cycle, and the information from each of these was recorded by the computer. At lower energies, where the computer was not able to hold all the available data, the number of muons was determined through the number of T and L triggers, which were recorded irrespective of whether or not they initiated a data-acquisition cycle.

The amount of beam scraping was recorded via two Čerenkov counters located close to the beam pipe, 140 ft and 190 ft upstream of the target.

Scraping occurring downstream of the Čerenkov counters was monitored by comparing the readings in the upstream secondary emission chamber with the downstream vertical plates.

In addition to the data recorded at the end of each AGS cycle, the computer also periodically recorded various items of bookkeeping information on magnetic tape. The target density, the currents in the precession coil and in the 6-ft-long bending magnet, and the amount of steel in the muon beam, were recorded. There was also a provision for entering comments onto the data tape.

D. On-Line Analysis

After writing the data on magnetic tape, the computer then checked the data in its memory to make sure that the number of incident protons was about as large as expected, and that the scraping was below certain limits. Currents in the beam magnets were also checked. Finally, the computer processed the raw data so that information on the hardware and the physics was available to the experimenters.

Hardware information included counts of the number of pulses from each scintillation counter, and the time distribution of the incident muons with respect to the AGS cycle. The most useful information was an oscilloscope display of the raw data, which was presented in a manner permitting a rapid but efficient visual check of the experiment. The redundancy of the information from the 0.1-μsec clock and from the "electron" pulses from the detector was also useful in checking the consistency of the data.

The data for a given trigger were interpreted in a straightforward manner. Since the detection of pulses from the counters was very efficient, a "$5\bar{3}$" pattern almost always pointed to the aluminum slab where a muon either stopped or scattered out of the detector. Electrons emitted in muon decay have a maximum energy of 53 MeV. The mean range for such electrons in aluminum is 2.3 in.,[35] so very few electrons passed through more than one scintillator. Only the scintillator immediately upstream or the scintillator immediately downstream of the appropriate aluminum slab was associated with a clock recording a time less than the clock limit of 12.7 μsec (See Fig. 6). From such data, the computer derived lifetime and polarization information. Data which did not satisfy the above criteria were labeled according to which criterion was not satisfied; the number of such failures was then accumulated.

Information on the flux, lifetime, and asymmetry was available from either oscilloscope displays or teletype listings. Further, the computer also performed least-squares fits to the data to estimate the muon lifetime and the magnitude of the muon decay asymmetry.

IV. ANALYSIS

A. General Procedure

The data were divided into "runs," defined by the muon's energy and sign, and by the density of the uranium target. In addition, a number of runs were made with different counter and logic configurations in order to test the detector and obtain information on the location and origin of the muons. These tests indicated that the muon flux was centered on the detector and that it originated near the uranium target.

The muon energy was determined by computing the energy lost in the degrader, assuming that the muons were produced at a depth of ≈ 1 interaction length in the uranium target, and that they stopped near the center of the detector. Values of dE/dx, the rate of energy loss, were computed from standard formulas,[36] and agreed with similar values that have recently been published.[37]

Data for each run were checked by plotting the ratios of the proton and muon monitors, taken one with another, against time. Scatter plots were made for pairs of monitors in order to check their linearity. A representative sample of the data was examined "by hand" as a further test for instrumental errors. Data for similar runs were then compared in order to obtain an estimate of any long-term variations in the monitors. Measurements of the muon flux were found to be reproducible within ±3%.

B. Muon Flux

1. *Detector Acceptance*

In order to compare the measured flux of muons due to meson decay with the flux expected from estimates[29,30] of the meson spectra, it was necessary to determine the acceptance of the detector, where acceptance is defined as the ratio

$$\frac{\text{number of } L \text{ or } T \text{ triggers}}{\text{total number of muons in the energy interval covered by the detector}}.$$

The acceptance was determined with the aid of a Monte Carlo computer program which traced the trajectory of muons through the degrader, the trigger counters, and the detector. The effect of small-angle scattering due to collisions was simulated with a Gaussian distribution,[38] and the effect of

large-angle scattering from the Coulomb field of the nucleus was handled by computing the momentum transfer corresponding to a randomly selected impact parameter. The root-mean-square angle of scattering given by the Monte Carlo results agreed with that given by an analytic calculation.

In addition, the ratio

$$\frac{L}{T}=\frac{\text{number of } L \text{ triggers}}{\text{number of } T \text{ triggers}}$$

was obtained from the Monte Carlo results and compared with the value observed in the experiment. Both the detector acceptance and the ratio L/T are sensitive to the initial angular distribution assumed for the muons. At 11.6 GeV, Monte Carlo results based on the meson spectra developed by Sanford and Wang[29] gave values of the ratio L/T which agreed with experimental results within the 10% statistical accuracy of the Monte Carlo program. At the three highest energies, a spectrum which fell off somewhat more rapidly with angle than the Sanford-Wang spectrum gave similar agreement.

Comparisons were also made between the detailed predictions of the Monte Carlo program and the data. The fraction of muons which produce a trigger (T or L) but do not enter the detector, and the fraction of muons which enter the detector but scatter out before stopping, can be predicted. This latter number, multiplied by the fraction of muon-decay positrons which escape the aluminum to produce a signal in the scintillator, allowed the fraction of "$\overline{53}$" events which should contain no decay positrons to be computed. Both calculated numbers were in agreement with the experimental results.

It is important to consider the straggling in the range of the muons. An estimate was obtained by extending previous results,[36,39] which cover muons with energies up to 11.3 GeV. The distribution in range R differs only slightly from a Gaussian form, with a width $\Delta R/R \simeq 5.5\%$ at 11.6 GeV. The straggling increases to 6.7% at 25.1 GeV. At the three highest energies, the smearing of the muon spectrum due to straggling increases the number of meson-decay muons which are in the energy range covered by the detector by a factor of two, since the number of pions produced per unit energy falls rapidly with increasing energy. At 11.6 GeV, straggling has little effect since the pion spectrum as a function of energy is nearly constant. For W-produced muons, the effect of straggling will be small, since the straggling is comparable to the thickness of the detector and, as shown in Fig. 5, the muon spectrum does not vary too rapidly with energy at 25 GeV.

2. *Corrections to Flux Measurements*

The flux of promptly produced muons is determined by extrapolating the plot of muon flux versus inverse target density. However, the measured muon flux must be corrected for proton and meson interactions in the non-target material in the beam, for the different solid angles subtended by the detector at the three targets, and for the "granularity" of the uranium target.

Since the target is not infinitely thick, material in the beam both upstream and downstream of it will contribute to the muon flux. The appropriate proton interaction lengths for each type of material have been determined experimentally.[40] The pion mean free paths are larger than those of the proton, since the pion-nucleon cross section is smaller than the nucleon-nucleon cross section. It was estimated that $\lambda_\pi \simeq 1.15\lambda_p$. The probability that a π^+ will escape the nucleus in which it is produced decreases as the nuclear size increases. It has been estimated[41] that nucleons in uranium might be $\frac{1}{3}$ as "efficient" as those in beryllium in producing high-energy mesons. Appropriate efficiencies were assigned to nuclei lying between beryllium and uranium on the basis of this estimate. The data were corrected so that they corresponded to the muon fluxes expected from protons directly incident on an infinitely thick uranium target. It was found that approximately 16% of the muon flux observed at the maximum target density did not originate in the target. The corresponding figures for the density-$\frac{1}{2}$ and density-$\frac{1}{3}$ targets are 7% and 4%. The 16% correction to the flux is estimated to be correct within ±3%.

The density-$\frac{1}{2}$ target begins 20 in. and the density-$\frac{1}{3}$ target begins 40 in. upstream of the maximum-density target. The respective solid angles are 3% and 7% lower than the solid angle subtended by the density-1 target. The corrections for target granularity are 0.7% for the density-$\frac{1}{3}$ target and 0.5% for the density-$\frac{1}{2}$ target.

Corrections to the flux data were also made in order to take into account the background due to muons of the "wrong" sign which were scattered into the detector. The wrong-sign background was determined by including an appropriate term in the functions used to fit the polarization and lifetime data (see Sec. IV D). The largest correction occurs at the highest energies, where 20% of the nominal μ^- data came from μ^+ flux. The μ^- contamination of the μ^+ data was negligible at all energies.

The flux of incident particles was low enough so that corrections for accidental coincidences were negligible.

3. *Comparison with Muon Flux Expected from Meson Decay*

The muon flux which originates in meson decay is obtained from the experimental data by subtracting

any "prompt" contribution to the flux. This flux may also be estimated by integrating the parametrizations of the meson spectra over appropriate regions of energy and angle. Comparison of the experimental result with the predictions at 11.6 GeV, in a region where the meson spectrum is well known, gives a check of many steps in the analysis of the data. At the highest energies, where no measurements of the meson spectra have been made, the experimental results permit a qualitative test of the parametrizations.

To make the comparison, the differential cross sections for pion and K-meson production at each energy were summed over angle in order to match the spectrum used by the Monte Carlo program, which determined the acceptance of the detector. The fraction of pions which decayed into muons with energies in the region covered by the detector was then computed. The effect of straggling was included in this calculation. The contributions were then summed over energy. The fluxes of muons thus computed corresponded to production in proton-beryllium collisions, and were multiplied by $\frac{1}{3}$ to obtain the fluxes expected from proton-uranium collisions. These fluxes, multiplied by the acceptance of the detector, are presented in Fig. 7, together with the experimental measurements. At the lowest energy, the agreement is fair, with the experimental results lying between the predictions of the two models. At the highest energies, the data indicate that the meson fluxes fall off more rapidly with energy than is indicated by the models of Sanford and Wang, and Hagedorn and Ranft.

C. Muon Polarization

1. *The Distribution of the Decay Electrons*

The relation between the longitudinal polarization of the muons and the forward-backward asymmetry in the decay electrons is established by integrating the spectrum over the aluminum slab. Neglecting radiative corrections and neglecting the finite mass of the electron, the spectrum for the decay of muons,

$$\mu^{\pm} \rightarrow e^{\pm} + \nu_{\mu} + \nu_{e},$$

with average polarization P, has the form

$$\frac{d^2N_{e^{\pm}}}{d(\cos\theta)dx} = I(x)[1 \pm PA(x)\cos\theta],$$

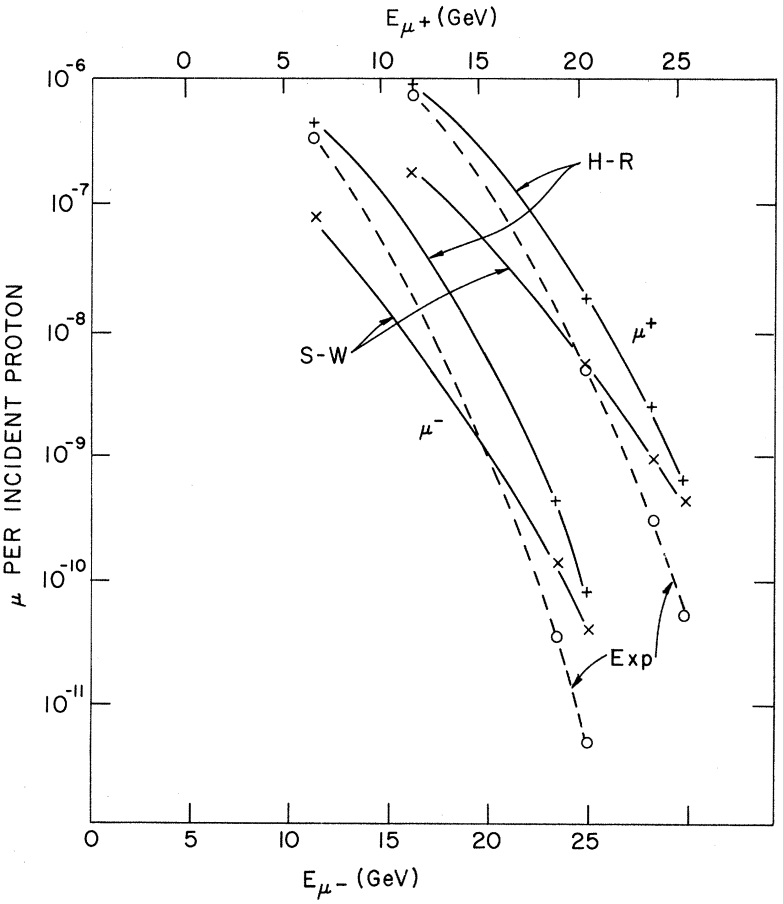

FIG. 7. The measured flux of positive and negative muons, per incident proton, is plotted as a function of muon energy. The fluxes expected on the basis of the Sanford-Wang and Hagedorn-Ranft spectra, integrated over the angular and energy regions covered by the detector, and corrected for the effects of multiple scattering and straggling, are also shown. The agreement is fair at 11.6 GeV. At the higher energies, the experimental results suggest a lower muon flux than that predicted by the two parametrizations.

where $I(x)=6x^2-4x^3$ and $A(x)=(x-\frac{1}{2})/(\frac{3}{2}-x)$. Here, θ is the angle between the electron momentum and the muon spin, and x is the ratio between the electron energy and the maximum electron energy, 53 MeV. The function $A(x)$ has its maximum value at $x=1$, decreases with lower electron energy, and finally changes sign for $x<\frac{1}{2}$. Hence, although only 20% of the decay positrons emerge from a slab, the high-energy positrons that do escape are quite asymmetric. The polarization information conveyed by this large asymmetry nearly equals that lost due to the lower statistics, while permitting the use of a detector that covered a large energy interval.

It was calculated that positively charged muons which had longitudinal polarization +1 and which stopped in a 4-in.-thick aluminum slab would have a front-to-back ratio, in the absence of a precession field,

$$\frac{N_F}{N_B}=\frac{\text{number of forward positrons}}{\text{number of backward positrons}}=1.76\pm0.06, \tag{5}$$

$$N_F=\int\frac{d^2N_e}{d(\cos\theta)dx}W_F(x,\cos\theta,z)dxd(\cos\theta)dz. \tag{6}$$

The integral was weighted by the probability $W_F(x,\cos\theta,z)$ that an electron produced at a depth z in the slab, at an angle θ, and with energy x, will escape in the forward hemisphere. The muon polarization was assumed to be directed along the beam axis and, hence, perpendicular to the plane of the slab. The polarization vectors of individual muons do not, in general, lie exactly along this line, due to the effects of multiple scattering. But on the average, the muon polarization will coincide with the beam axis, and the effect of the multiple scattering will appear as an over-all depolarization, whose effects were considered in the analysis. The energy loss due to bremsstrahlung and pair-production, and the multiple scattering of the positrons, were included in W_F. The expression for N_B was calculated in a similar fashion.

Negatively charged muons which stop in aluminum[42] enter atomic orbits and rapidly lose their polarization. Further, 60% of the negative muons which stop are captured by the nucleus before decaying. Thus, only about 8% of the μ^--decay electrons are observed, with an asymmetry near zero.

2. *Depolarization Effects*

High-energy muons are slightly depolarized when scattered by the nuclear Coulomb field. The muon experiences a field which is partly electric and partly magnetic, and is depolarized when it is slow enough to be scattered by the electric field but still fast enough to see a magnetic field, to which its magnetic moment is coupled. No depolarization occurs at very high energies or at very low energies. The formula[43] for the depolarization has been given as

$$P=P_{\text{meas}}/(1-\delta_1),$$

where

$$\delta_1=\frac{3}{2}\frac{E_s^2}{p_1}\left(1-\frac{1}{3}\frac{M_\mu}{p_1}\right)\frac{1}{X_0}\frac{R}{p_0},$$

where $E_s=21$ MeV, X_0 is the radiation length of the degrader, R is the muon range, and p_0 is the initial momentum. The value of p_1, the cutoff momentum at which the muon becomes nonrelativistic and no longer sees a magnetic field, is $\gtrsim M_\mu$, although it is difficult to determine precisely. We have taken $p_1=236$ MeV/c, and obtained the depolarization that occurs during the remainder of the muon's range from experimental measurements[44] of the polarization of muons which are produced with polarization -1 in the decay $K^+\to\mu^++\nu$, and which stopped in aluminum. The average of these experimental measurements is

$$P=(1.04\pm0.08)P_{\text{meas}}.$$

For $p_1=236$ MeV/c, $\delta_1=0.09\pm0.01$. Combining these results, the muon depolarization due to Coulomb scattering in the degrader is then estimated to be

$$P=(1.14\pm0.09)P_{\text{meas}}.$$

The nonuniformities in the magnetic field applied to the detector cause the spins of the muons to pre-

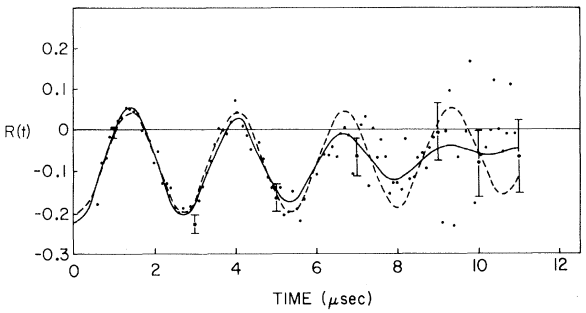

FIG. 8. The measured asymmetry in the decay positrons,

$$R(t)=[F(t)-B(t)]/[F(t)+B(t)],$$

where $F(t)$ and $B(t)$ are the numbers of positrons observed in the forward and backward hemispheres (relative to the direction of the incident muons) at a time t, is plotted as a function of time for the sample of data used to determine the depolarization due to the nonuniformities in the precession field. The best-fit curves, with or without provision for a depolarization with time, are also shown. The data are typical of those taken in the experiment.

cess at slightly different frequencies. Thus, the measured polarization shows a decrease with time. The effect was estimated by assuming that the nonuniformities caused the precession frequencies to be distributed uniformly in a band $\Delta\omega$ around the average frequency ω_0. Values of ω_0 and $\Delta\omega$ may be estimated from the geometry of the coils used to produce the field, and then compared with those determined by fitting the data with this hypothesis. The two values for ω_0 differed by only a few percent. The value of $\Delta\omega$ determined from the data was $(25 \pm 12)\%$, somewhat larger than the 15% spread that was expected. The least-squares fit to the data, with and without the depolarization term, is shown in Fig. 8, along with the sample of data used to determine the values of ω_0 and $\Delta\omega$.

It has been demonstrated experimentally that μ^+ undergo no depolarization due to microscopic magnetic fields in aluminum.[45]

3. *Analysis of Polarization and Lifetime Information*

The data were fitted, by the method of least squares, to functions which made provision for contributions from the decay of polarized muons in scintillator and in aluminum, for a small depolarization with time, and for backgrounds due to random counts or muons of the wrong sign. The constant background was determined, from a fit to the data, to be $\approx 0.1\%$ of the signal at $t = 0$.

The background due to muons of the "wrong" sign which were scattered into the detector was determined from the fit to the μ^- data. The μ^+ contamination of the μ^- data was 20% at 25.1 GeV, decreasing to 5% at 11.6 GeV. This information, together with the measurements of charge ratios, enabled the μ^- contamination of the μ^+ flux to be calculated as $\approx 0.2\%$.

The lifetimes of the positive and negative muons in aluminum were determined from the least-squares fit to the data to be 2.26 ± 0.02 μsec for μ^+ and 0.90 ± 0.05 μsec for μ^-, where only statistical errors were considered. These are to be compared to the accepted values, 2.1983 ± 0.0008 μsec and 0.865 ± 0.004 μsec, respectively.[29,46]

4. *Average Polarization of Muons Originating in Meson Decay*

Positive muons produced in meson decay, which are emitted in the beam direction as determined in the meson center-of-mass system, have a polarization of -1 with respect to the beam direction. However, not all of the muons which stop in the detector were directed forward in their decay, so the average polarization is not quite -1. The component of the muon polarization in the direction of its laboratory momentum has been calculated[43] to be

$$(EE^* - \gamma_\pi M_\mu^2)/(pp^*),$$

where (E^*, p^*) and (E, p) are the four-momenta of the muon in the pion center-of-mass system and in the laboratory, respectively, and γ_π is the laboratory energy of the pion divided by its mass. The average polarization was obtained by integrating this factor over the pion and K-meson spectra and then dividing by the meson flux. For kaons, the pion mass is replaced by the kaon mass in determining the average value of the polarization. The average polarization of muons from meson decay was estimated to be 0.86 ± 0.05, 0.83 ± 0.05, 0.77 ± 0.05, and 0.64 ± 0.03 for muons of energy 25.1, 23.5, 20.5, and 11.6 GeV, respectively. The errors reflect the uncertainties in the meson spectrum, which appears to fall off more rapidly with energy near the kinematic limit than indicated by the parametrization of Sanford and Wang.

Experimentally, the polarization of muons originating in meson decay may be determined from the measured polarization if the contribution due to the prompt flux can be estimated. The values of the polarization determined in this fashion are compared to the predictions of the Sanford-Wang para-

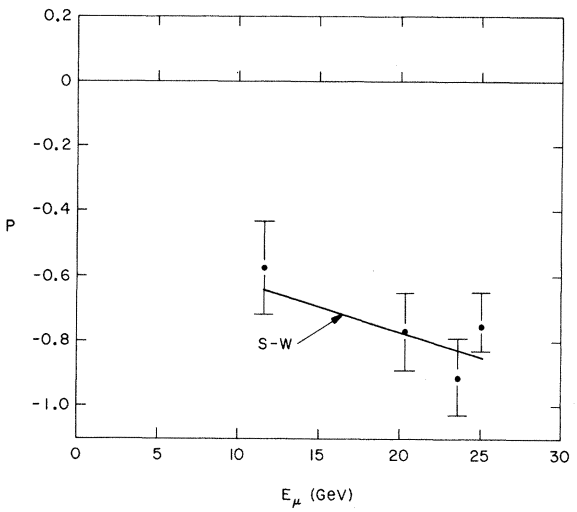

FIG. 9. The polarizations P, measured at target density $\frac{1}{3}$ and corrected for contributions due to the flux of prompt muons and for the depolarization in the degrader, are plotted as a function of muon energy. They are compared to the predictions of the Sanford-Wang parametrization for the average polarization of muons originating in the decay of positive pions and kaons and detected by our apparatus. The uncertainties in the estimates based on the Sanford-Wang formulas are not shown; they are estimated to be ± 0.05 at the three highest energies, and ± 0.03 at 11.6 GeV. The data at target density $\frac{1}{3}$ are the least sensitive to errors in estimates of the contribution due to the prompt flux. The errors shown include both statistical and systematic uncertainties.

metrization in Fig. 9. The data taken with the target density equal to $\frac{1}{3}$ are the least sensitive to errors in the estimates of the prompt flux and were used in the comparison.

V. RESULTS AND CONCLUSIONS

A. Measurements of the Muon Flux

The measurements of the muon flux were corrected so as to correspond to the flux of muons of one sign produced by a proton beam striking an infinitely thick uranium target and detected by our apparatus. These measurements were converted to values of the cross section for muon production, $\delta\sigma_\mu$, by relating $\delta\sigma_\mu$ to the total inelastic proton-nucleon cross section, $\sigma_{\text{inel}} \cong 28$ mb.

$$\delta\sigma_\mu = \left(\frac{\text{number of incident protons which produce muons}}{\text{number of incident protons}}\right)\times\sigma_{\text{inel}}$$

$$= (\text{number of muons per incident proton})\times\sigma_{\text{inel}},$$

since all protons will eventually undergo an inelastic interaction. The data were then normalized to the momentum interval ($\approx$1.4 GeV/c) and angular interval (1.17×10^{-3} sr, in the laboratory) covered by the detector. The data for muons with a particular energy and sign, plotted against the inverse target density, were fitted to a straight line, which was extrapolated to infinite target density as shown in Fig. 10.

The positive and negative muon fluxes obtained from the extrapolation to infinite target density were interpreted as a flux of "prompt" muon pairs, with a small background due to mesons produced by the proton beam striking the vacuum pipe upstream of the target. The flux data do not contain substantial evidence for W production. Taking the differ-

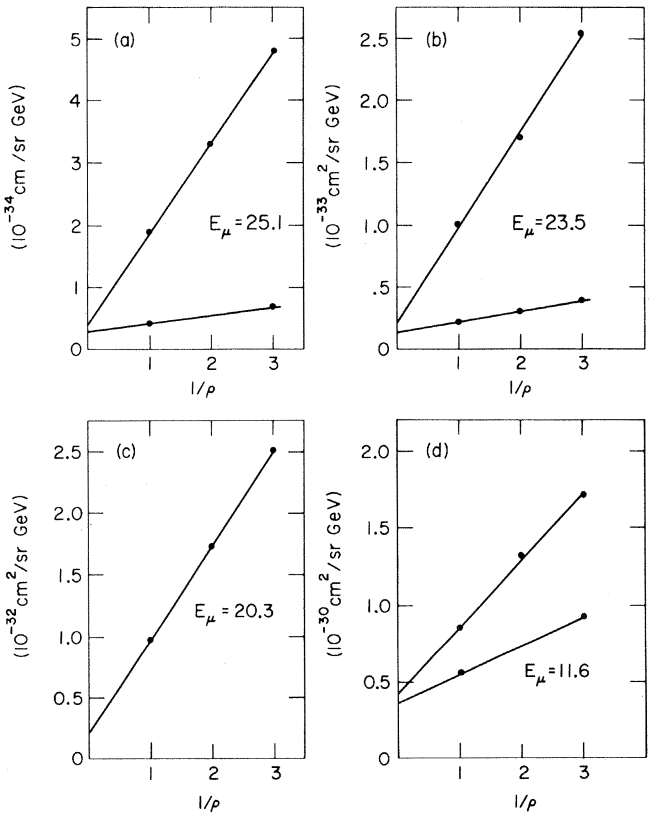

FIG. 10. The fluxes of positive and negative muons are plotted as a function of inverse target density for each of the four muon energies. The measured fluxes have been corrected to correspond to muons produced in infinitely thick uranium targets, as discussed in the text. No μ^- data were taken at 20.3 GeV. The errors in the fluxes are $\approx$3%, only slightly larger than the data points. The energy E_μ is measured in GeV and the density ρ is measured in units of the density of uranium.

ence between the positive and negative fluxes as an upper limit for W production, we have

$$B\frac{d^2\sigma_W}{dEd\Omega} \lesssim 1.5\times10^{-35}\ \text{cm}^2/(\text{sr GeV}).$$

Limits on the total cross section for W production may be obtained if the model used to calculate W production is used to interpret the limit on the differential cross section. These limits, which are a function of the mass of the W, are presented in Fig. 11. For masses in the range 2 to 4.5 GeV/c^2, we have, approximately,

$$B\sigma_W \lesssim 6\times10^{-36}\ \text{cm}^2.$$

B. Measurements of the Muon Polarization

A typical plot of the measured asymmetry in the positron distribution,

$$R(t)=\frac{N_F(t)-N_B(t)}{N_F(t)+N_B(t)},$$

versus time, is presented in Fig. 8. The precession of the polarization with time and the bias due to muons stopping in the scintillator are evident. The amplitude S of the cosine wave in the plot is the asymmetry (at time $t=0$) due to the decay of muons which stopped in aluminum. The amplitudes were determined from the least-squares fits to the data at each muon energy and uranium target density. The phases of the cosine functions were found to be 180°, indicating that the polarization was longitudinal and that the average polarization of the incident muon flux was negative. The muon polarizations were obtained from the values of S by normalizing to the asymmetry which was calculated [Eq. (5)] for muons with polarization +1 stopping in a 4-in. aluminum slab,

$$\frac{N_F-N_B}{N_F+N_B}=0.275\pm0.023,$$

and then correcting for the muon depolarization in the degrader. The μ^+ polarizations at each energy and target density are presented in Fig. 12.

It is possible to test for the presence of muons from W decay or from the electromagnetic decay of neutral particles by comparing the measured polarization with that expected for muons originating in meson decay. However, the uncertainties in the meson spectrum and in the depolarization correction make this procedure insensitive to a flux of muons with polarization 0 or +1, which is small in comparison with the flux of muons with polarization −1. A more sensitive test for the existence of such muons may be made by comparing the measurement of S made at target density 1 with the measurement made at density $\frac{1}{3}$. The data at the highest energy are, of course, the most sensitive to the presence of muons with polarization 0 or +1. For the data at 25.1 GeV,

$$S=-0.20\pm0.02 \quad \text{for density 1,}$$

$$S=-0.18\pm0.02 \quad \text{for density } \tfrac{1}{3},$$

where the phase of the cosine term is denoted by the minus sign. These measurements are the same, within errors, and contain no evidence for the production of W's or muon pairs. The sensitivity of the asymmetry measurement is fixed by the accuracy with which the two values of S were determined, 10%. Thus, the polarization is sensitive to a flux of muons from W decay which is as small as 10% of the flux of muons from meson decay, and to a flux of muon pairs which is as small as 20% of the meson-decay flux. The polarization data are consistent with the measurements of the muon flux, although somewhat less sensitive to the presence of W's and muon pairs.

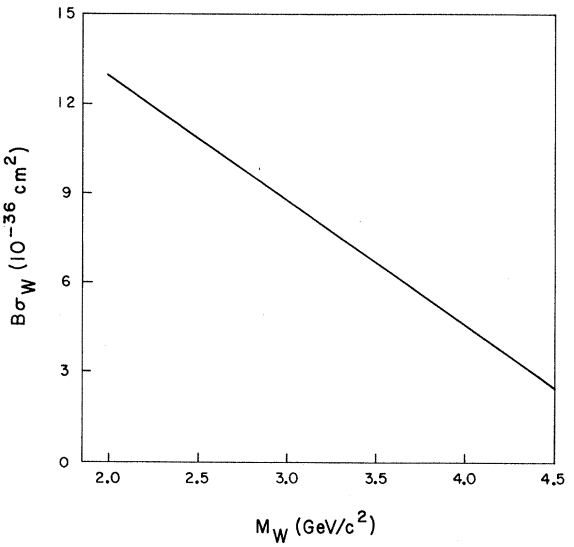

FIG. 11. The results of the experiment, interpreted in terms of our model for W production, have been used to obtain upper limits on $B\sigma_W$, the branching ratio for muon decay times the total cross section for W production. The limits on $B\sigma_W$ are plotted as a function of a M_W, the mass of the W.

C. Muon Charge Ratios

The ratios of the flux of positive muons to negative muons were obtained from the density-$\frac{1}{3}$ data after subtraction of the flux due to muon pairs, and are plotted in Fig. 13. The ratios show an expected rise with muon energy, indicating an increase in the relative difficulty of producing a negative meson as one approaches the kinematic limit. The ratios expected on the basis of the Sanford-Wang and Hagedorn-Ranft models are also shown.

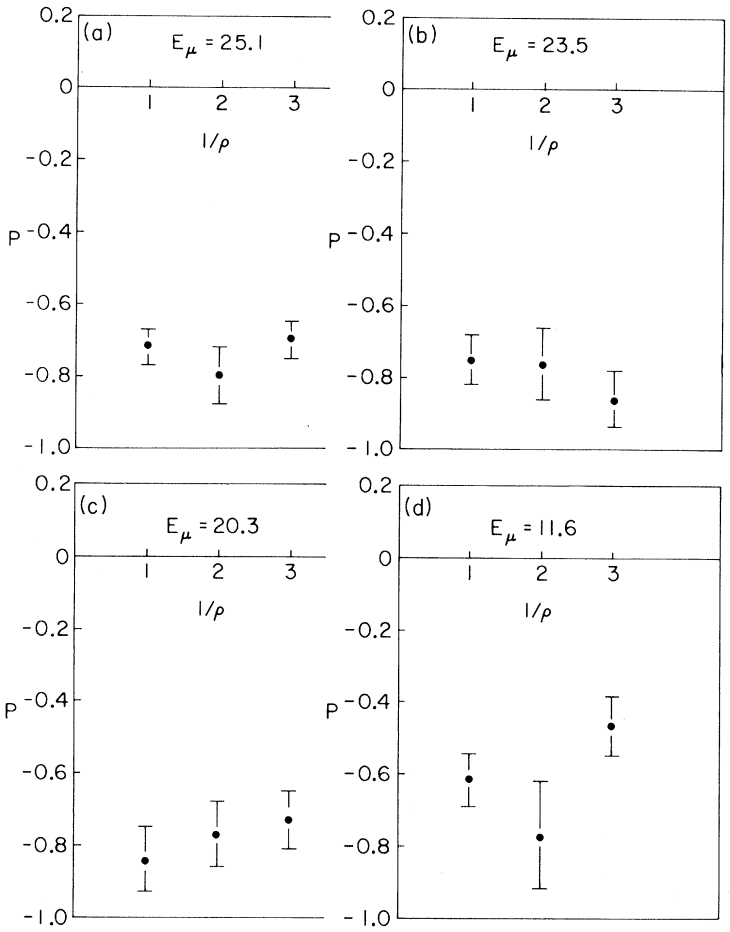

FIG. 12. The polarization P of muons detected in the experiment, corrected for depolarization in the degrader as discussed in the text, is plotted at each muon energy as a function of inverse target density. The energy is measured in GeV and the density in units of the density of uranium. The errors shown include both statistical and systematic erors in obtaining P.

The agreement is good at 11.6 GeV, but not at the highest energies.

D. Muon Pairs

We feel that the existence of a flux of negative muons at the infinite-density intercept in Fig. 10, which is a large fraction of the flux of negative muons at density 1, is good evidence for the detection of muon pairs. Any background due to "scraping" of the proton beam can be seen from the data (Fig. 10) to be a small portion of the positive muon flux at density 1. Since the μ^+/μ^- ratios at the highest energies are large (Fig. 13), such a background will only be a small part of the μ^- "prompt" flux also. We conclude that the majority of the μ^- "prompt" flux is due to muon pairs.[47]

Values for the flux resulting from muon pairs are presented in Fig. 14. They were obtained by analyzing the positive and negative "prompt" muons in terms of a flux of muon pairs, with a small "scraping" background having the same charge ratio as the muons from the decay of mesons produced in the uranium target (Fig. 13). No μ^- data were taken at 20.3 GeV, so only an upper limit on the production of muon pairs is available. The implications of the flux data taken at 11.6 GeV in terms of a flux of muon pairs [Fig. 10(d)] are not in good agreement with the polarization measurements made at that energy [Fig. 12(d)], which show no evidence of a flux of muon pairs comparable to the meson-decay flux at maximum target density. Since the measurements at 11.6 GeV were necessarily made without the massive shielding available at the highest energies, counting rates were very high, resulting in certain instrumental difficulties, and the discrimination against muons produced by beam scraping upstream from the target was reduced. We feel, then, that our measurement of a rather large "prompt" flux at this energy might not be completely reliable,

and we do not wish to draw any conclusions concerning the production of muon pairs from the data at this energy. However, the polarization data do indicate that any contribution to the flux from electromagnetic processes must be a small fraction of the total muon flux from the most dense target.

E. Implications in Terms of the Existence of a W

We do not believe that the negative results of the experiment can be taken as evidence against the existence of W's with a mass less than 4 GeV/c^2. This is readily seen using the relation obtained by Yamaguchi between the flux of muons from W decay and the flux of muon pairs from the decay of massive virtual γ's [Eq. (4)]. Even with a rather broad invariant-mass acceptance, we see few prompt muons from all sources at 0°. Then the W production of muons, which should be small compared to the electromagnetic production of muons, is certainly very small. Although it was possible to improve the resolution in invariant mass of the source particle, W or virtual photon, and then discriminate more sharply against electromagnetically produced muons, this was not done as the 0° measurements established that the W flux was too small to detect.

This same conclusion is reached if the experimental data are viewed in terms of our model for W production. It can be seen from Fig. 14 that, at 25.1 GeV, our estimates of the flux of muon pairs were overly optimistic by a factor of 5. If our estimates of W production are reduced by a corresponding amount, the fluxes of decay muons are then too low to be observed in this experiment.

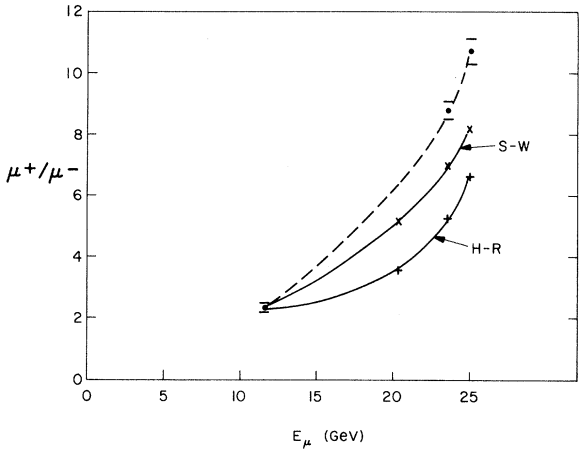

FIG. 13. The charge ratio μ^+/μ^- of muons originating in meson decay, obtained by correcting the experimental data at target density $\frac{1}{3}$ for contributions due to the "prompt" flux of muons, is plotted as a function of muon energy. The predictions of the Sanford-Wang and Hagedorn-Ranft parametrizations, adapted to our experimental arrangement, are also shown. No μ^- data were taken at 20.3 GeV.

F. Limit of the X Process

We can express the contribution of the X process in terms of the ratio of the intensity of muons produced by this process to the intensity of pions produced at the same energy. Only pions with an incident energy greater than the energy of the muons which are detected can contribute to this muon flux. About 10^{-4} of these pions decay to muons before interacting in the shield, and the muons from these decays have an energy spread extending from the full energy of the pion to about 60% of the energy of the pion. When the spectrum of the pions produced in the interactions is considered together with the muon spectra from those pion decays, the contribution from pions is reduced another factor of 10, and the ratio of pions produced to muons observed at a uranium target of density 1 is about 10^5. The fraction of the residual muons at infinite target density to the muons at density 1 is $\frac{1}{6}$, and if we attribute all the residual muons to the X process, we find that its contribution is less than 2×10^{-6} of

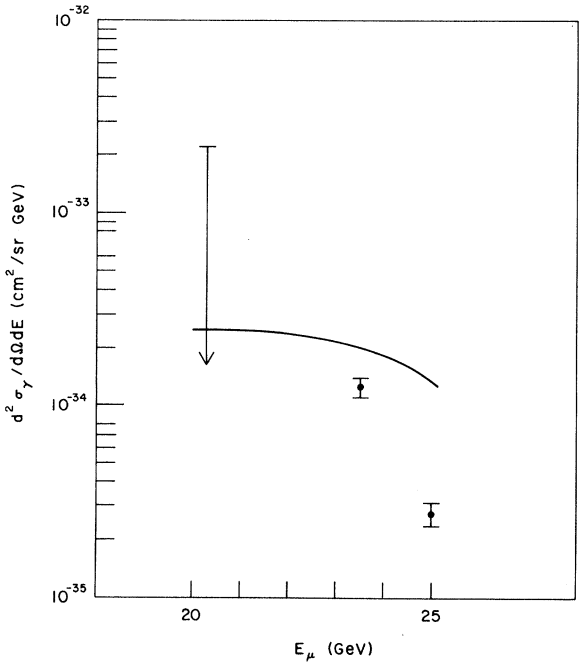

FIG. 14. The flux of muon pairs, obtained from the experimental data, is plotted as a function of muon energy. The predictions of our model for the production of heavy virtual γ's and the detection of one of the subsequent decay muons are shown as the solid line. At 25.1 GeV, it is seen that the prediction is higher than the measured flux by a factor of ≈5. Since no μ^- data were taken at 20.3 GeV, only an upper limit is available at that energy.

the pion flux. This is to be compared to the ratio of about 2×10^{-2} found in cosmic rays.[17] It seems, however, that the residual muon intensity is quite consistent with that intensity expected from electromagnetic production, and the limit on any otherwise unknown X process is lower yet.

Christenson *et al.* have now published[47] a very interesting set of measurements concerning the production of muon pairs of large invariant mass by the interaction of high-energy protons. They point out that their results, together with the CVC relations [Eq. (4)], suggest that a W of mass 2 GeV/c^2 could be expected to be produced with a cross section of 4×10^{-35} cm^2, where B is expected to be about equal to 4. This shows that our experiment was probably barely sensitive to W production for a W mass of 2 GeV/c^2, and that our conclusion that it was not sensitive for larger masses was correct.

---

*Work performed under the auspices of the U. S. Atomic Energy Commission.

†Now at the University of Indiana, Bloomington, Ind.

‡Now at Cornell University, Ithaca, N.Y.

§Now at the National Accelerator Laboratory, Batavia, Ill.

[1]T. D. Lee and C. N. Yang, Phys. Rev. Letters 4, 307 (1960); Phys. Rev. 119, 1410 (1960).

[2]P. J. Wanderer, Jr. *et al.*, Phys. Rev. Letters 23, 729 (1969).

[3]G. Bernardini *et al.*, Nuovo Cimento 38, 608 (1965).

[4]R. Burns *et al.*, Phys. Rev. Letters 15, 42 (1965).

[5]R. Cowsik and Y. Pal, Tata Institute of Fundamental Research Report No. NE-69-7 (unpublished); in Proceedings of the Eleventh International Conference on Cosmic Rays, Budapest, 1969 (unpublished).

[6]R. Burns *et al.*, Phys. Rev. Letters 15, 830 (1965).

[7]R. Burns *et al.*, Columbia University Nevis Laboratories Report No. NEVIS-153, 1966 (unpublished).

[8]R. C. Lamb *et al.*, Phys. Rev. Letters 15, 800 (1965).

[9]Y. Yamaguchi, Nuovo Cimento 43A, 193 (1966).

[10]F. E. Low, Comments Nucl. Particle Phys. 2, 33 (1968).

[11]R. E. Marshak, Riazuddin, and C. P. Ryan, *Theory of Weak Interactions in Particle Physics* (Wiley-Interscience, New York, 1969).

[12]H. Foeth *et al.*, Phys. Letters 30B, 282 (1969); A. R. Clark *et al.*, Lawrence Radiation Laboratory Report No. UCRL-20078 (unpublished) and private communication.

[13]N. R. Mohapatra, J. Subba Rao, and R. E. Marshak, Phys. Rev. 171, 1502 (1968).

[14]B. L. Ioffe, Zh. Eksperim. i Teor. Fiz. 47, 975 (1964) [Soviet Phys. JETP 20, 654 (1965)].

[15]C. Ryan, S. Okubo, and R. E. Marshak, Nuovo Cimento 34, 753 (1964).

[16]A theory of weak interactions, involving several intermediate bosons but without divergences, has recently been proposed. Here too, the typical boson mass suggested by second-order weak processes is about 2 to 8 GeV/c^2. See M. Gell-Mann, M. L. Goldberger, N. M. Kroll, and F. E. Low, Phys. Rev. 179, 1518 (1967).

[17]T. W. Keuffel, T. L. Osborne, G. L. Bolingbroke, G. W. Mason, M. O. Larson, G. H. Lowe, T. H. Parker, R. O. Stenerson, and H. E. Bergeson, in Proceedings of the Eleventh International Conference on Cosmic Rays, Budapest, 1969 (unpublished).

[18]G. G. Bunatyan *et al.*, Zh. Eksperim. i Teor. Fiz. Pis'ma v Redektsiyu 9, 325 (1965) [Soviet Phys. JETP Letters 9, 192 (1969)].

[19]T. D. Bjorken, S. Pakvasa, W. Simmons, and S. F. Tuan, Phys. Rev. 184, 1345 (1969).

[20]G. F. Chew and F. E. Low, Phys. Rev. 113, 1640 (1959).

[21]V. Namias and L. Wolfenstein, Nuovo Cimento 36, 542 (1965).

[22]M. Conversi, T. Massam, Th. Muller, and A. Zichichi, Nuovo Cimento 40A, 690 (1965); D. L. Hartill *et al.*, Phys. Rev. 184, 1415 (1969). For some general comments on nucleon form factors, see R. Wilson, Phys. Today 22, No. 1, 47 (1969); T. Massam and A. Zichichi, Nuovo Cimento 43A, 1137 (1966).

[23]E. D. Bloom *et al.*, Phys. Rev. Letters 23, 930 (1969); E. Breidenbach *et al.*, *ibid.* 23, 935 (1969).

[24]S. Drell and T. Yan, Phys. Rev. Letters 24, 181 (1970); 24, 855 (1970); S. Drell, D. Levy, and T. Yan, Phys. Rev. 187, 2159 (1969); Phys. Rev. D 1, 1035 (1970).

[25]R. P. Feynman, Phys. Rev. Letters 23, 1415 (1969).

[26]J. V. Allaby *et al.*, Phys. Letters 29B, 198 (1969).

[27]R. Omnes and M. Froissart, *Mandelstam Theory and Regge Poles* (Benjamin, New York, 1965).

[28]For example, the spread in the laboratory momentum of a W of mass 3 GeV/c^2 would be, typically, ±2%, which is small compared with the ±7% straggling in the range of the decay muons. Similarly, the smearing of the angular distribution of the muons due to the Fermi momentum is only 20% of that due to multiple scattering.

[29]J. R. Sanford and C. L. Wang, Brookhaven National Laboratory Accelerator Department AGS Internal Reports No. JRS/CLW-1 and JRS/CLW-2, 1967 (unpublished).

[30]R. Hagedorn and J. Ranft, Nuovo Cimento Suppl. 6, 169 (1968). The predictions of this model for 28-GeV p^+-Be collisions were supplied by M. Awschalom and T. White of the National Accelerator Laboratory [see NAL Internal Report No. FN-191, 2020, 1969 (unpublished)]. J. Ranft, Phys. Letters 31B, 529 (1970), gives a more recent version of the model. As noted in this article, the predictions of the older model for meson fluxes at energies near the kinematic limit were higher than observed, in agreement with the results of this experiment. Detailed predictions of the newer version were not yet available for use in the analysis here.

[31]Particle Data Group, Rev. Mod. Phys. 42, 87 (1970).

[32]G. Parzen, Brookhaven National Laboratory Accelerator Department Internal Report No. AADD-155, 1969 (unpublished).

[33]K. Jellett and G. Parzen, Brookhaven National Laboratory Accelerator Department Internal Report No. AADD-149, 1969 (unpublished).

[34]J. D. Fox (private communication).
[35]H. Bethe and J. Ashkin, in *Experimental Nuclear Physics*, edited by E. Segrè (Wiley, New York, 1953), Vol. I.
[36]R. M. Sternheimer, in *Methods of Experimental Physics*, edited by L. Marton, C. S. Wu, and L. C. L. Yuan (Academic, New York, 1961), Vol. 5A.
[37]P. M. Joseph, Nucl. Instr. Methods 75, 13 (1969).
[38]B. Rossi, *High-Energy Particles* (Prentice-Hall, Englewood Cliffs, N. J., 1952).
[39]R. M. Sternheimer, Phys. Rev. 117, 485 (1960).
[40]A. Ashmore *et al.*, Phys. Rev. Letters 5, 576 (1960).
[41]"200 BeV Accelerator Design Study," Lawrence Radiation Laboratory Report No. UCRL-16000, 1965 (unpublished).
[42]G. Feinberg and L. M. Lederman, Ann. Rev. Nucl. Sci. 13, 431 (1963).
[43]S. Hayakawa, Phys. Rev. 108, 1533 (1957).
[44]D. Cutts *et al.*, Phys. Rev. Letters 20, 955 (1968); Phys. Rev. 184, 1380 (1969); C. Coombes *et al.*, *ibid.* 108, 1348 (1957).
[45]A. Buhler *et al.*, Nuovo Cimento 39, 824 (1965); M. Weinrich, Columbia University Nevis Laboratories Report No. NEVIS-56, 1958 (unpublished); R. A. Swanson, Phys. Rev. 112, 580 (1958).
[46]M. Eckhause, R. T. Siegel, R. E. Welsh, and T. A. Filippas, Nucl. Phys. 81, 575 (1966).
[47]J. H. Christenson, G. S. Hicks, L. M. Lederman, P. J. Limon, B. G. Pope, and E. Zavattini, Phys. Rev. Letters 25, 1523 (1970).

PHYSICAL REVIEW D VOLUME 3, NUMBER 11 1 JUNE 1971

2130-MeV $\Lambda^0 p$ Mass Enhancement in the Reaction $K^- d \to \Lambda^0 p \pi^-$ at 1.45 and 1.65 GeV/c

D. Eastwood, J. R. Fry, F. R. Heathcote, and G. S. Islam
Department of Physics, University of Birmingham, Birmingham, United Kingdom

and

D. J. Candlin, G. Copley, and G. R. Evans
Department of Natural Philosophy, University of Edinburgh, Edinburgh, United Kingdom

and

J. R. Campbell, W. T. Morton, and P. J. Negus
Department of Natural Philosophy, University of Glasgow, Glasgow, United Kingdom

and

M. J. Counihan, D. P. Goyal, D. B. Miller, and B. Schwarzschild
Department of Physics, Imperial College of Science and Technology, London, United Kingdom
(Received 29 September 1971)

An enhancement in the $\Lambda^0 p$ mass spectrum from the reaction $K^- d \to \Lambda^0 p \pi^-$ at K^- momenta of 1.45 and 1.65 GeV/c is reported. The peak of the distribution occurs at $\simeq$2129 MeV and the width at half-height is $\simeq$10 MeV. A possible interpretation of this effect is given.

I. INTRODUCTION

Several groups[1-3] have reported an enhancement in the Λp mass distribution around 2130 MeV from a study of the reaction

$$K^- d \to \Lambda p \pi^- \qquad (1)$$

in a deuterium bubble chamber. Cline *et al.*[1] observed this effect by using K^- at momentum 400 MeV/c. The position of the peak in the Λp mass distribution was 2126 MeV, and the width was less than 10 MeV. Subsequently, Alexander *et al.*[2] reported the effect by using K^- at momenta 910, 1007, and 1106 MeV/c, but the peak in this case appears to be at $\simeq$2129 MeV, and the width is $\simeq$10 MeV. More recently, Tan[3] studied reaction (1) with stopping K^- and observed the enhancement, with the peak at $\simeq$2129 MeV and the width $\simeq$7 MeV. Although in all these experiments the enhancement is statistically significant, it is not yet clear whether this constitutes evidence for the existence of a Λp resonance, or whether the enhancement could arise from a kinematical effect involving an intermediate Σ hyperon, i.e.,

$$K^- d \to \pi^- (\Sigma N) \searrow \Lambda p. \qquad (2)$$

Detailed reviews of the observations and their interpretation were presented at the 1969 hypernuclei conference.[4]

In the present paper we report the observation of this enhancement in a study of reaction (1) at K^-